

ORIGINAL PAGE IS
OF POOR QUALITY

N82 23429

Hydrodynamic Performance of an Annular Liquid Jet: Production of Spherical Shells

James M. Kendall

Jet Propulsion Laboratory
Pasadena, CA 91109

Abstract

An annular jet flow of liquid surrounding a flow of gas at its core is extremely unstable. Axisymmetric oscillations arise spontaneously, and grow with such rapidity along the axial dimension that a pinch-off of the liquid and an encapsulation of the core gas occurs within as few as four jet diameters. The shells which result thereby may be described as thick-wall bubbles, for which van der Waals forces are unimportant. A description is given here of the fluid dynamic processes by which the shells are formed, and of means for preserving and promoting the geometrical symmetry of the product. The forming of metallic shells is mentioned.

Introduction

The investigation described here follows from considerations put forward by Messrs. T. G. Wang and D. D. Elleman of this Laboratory for the production of rigid, impermeable shells for various applications. They had noted during zero-G flights of the NASA KC-135 aircraft that free-floating drops of water containing a gaseous bubble spontaneously assumed a spherical and concentric form, suggesting that if the liquid were to solidify in such state there might result a product of some utility. They proposed a means for the mass-production of liquid shells within the laboratory, based upon the periodic cutting-off of lengths of a gas-core liquid jet, with concurrent sealing of the free ends by any of several methods which seemed promising. This author's earliest attempt to generate a suitable jet flow for evaluating the technique revealed immediately that the hollow jet was sufficiently unstable that the formation of shells needed no inducement.

Fig. 1 illustrates this. The upper figure there pertains to a 4.0-mm jet of water which accelerated downward under action of gravity. The three component photographs were obtained at stations separated axially by 1.0 m each, so that the observation extended over 2.0 m, or more than 500 diameters. The flow within the nozzle was intentionally rendered slightly periodic in order to stimulate the wave growth evident at the second and third stations on account of the well-known Rayleigh instability.¹ An important feature of the Rayleigh analysis, and of an experiment such as this, is that disturbances extending over a wide range of wave numbers are unstable, and that the growth of even the most unstable of these is quite slow, requiring hundreds of diameters for pinch-off under the present conditions. No single wave number is favored to the exclusion of all others. By contrast, the lower figure shows the same nozzle, except that a coaxial flow of air had been provided at the center of the jet. Again, there existed an axial growth of axisymmetric waves, but these grew to such magnitude that pinch-off, accompanied by encapsulation of the core gas, is to be observed at a station approximately four diameters from the nozzle. Most importantly, no perturbation was supplied in this case, yet the frequency stability of the cyclic process was exceedingly uniform, resulting in a corresponding uniformity in mass of the individual shell specimens. It is the formation of these which is the subject of the study to be described.

The work has been motivated jointly by scientific interest in the fluid motion, and by the potential utility of a method for the mass-production of rigid shells of high quality. One application for these concerns fusion target technology. There, it is sought to produce metallic shells of high precision and strength, and preferably composed of a metal of high average atomic number. Hendricks² has described some of the truly remarkable accomplishments of a program for the manufacture of multi-layer target shells.

Apparatus and techniques

Experiments have been carried out employing a number of different nozzles and operating fluids. Fig. 2 shows, on the left, the general configuration of a typical nozzle, other designs having differed from this principally with regard to dimensions and to mechanical details of alignment. Typical flow settings for this nozzle are included. Other nozzles incorporated nozzle exit diameters of 0.3, 0.66, and 2.0 mm. The principal features are the central tube through which the gas supply is introduced, the contour of the interior surface of the liquid-flow channel, and the passageway of liquid flow defined by the clearance between the gas tube and nozzle aperture. The performance was relatively insensitive to the gas-tube wall thickness and to the axial position of the gas-tube terminal end, but radial

ORIGINAL PAGE IS
OF POOR QUALITY

alignment was moderately important. On the right is shown the smallest nozzle tested, a millimeter scale being included. Water and glycerin served as the working liquids in performance tests, and liquid metals were also used as noted later. Test gasses included compressed air, helium, nitrogen and Freon-12. Liquid flow regulation was accomplished through adjustment of the free-surface elevation, or by gas-pressurization of the reservoir. The required pressure was equal to the sum of the pressure drop through the nozzle due to viscosity, plus the Bernoulli term. Gas flow control was accomplished by providing a fine capillary tube ahead of the gas supply tube in order to raise the supply pressure to a value easily measured and regulated.

Gas flow rates were determined by measurement of the pressure imposed upon the capillary resistor, the flow through which in turn had been calibrated against a wet test meter. Liquid flow rates were measured by capturing the stream of shells in a graduated cylinder for a precise duration. The frequency of shell production was determined stroboscopically or by measurement of the frequency of light-beam interruption. Shell diameters were measured optically under stroboscopic illumination using a traversing-mount telescope. Heat transfer to freely-falling shells was determined by measuring the temperature difference between that of heated water within the reservoir and that of shells captured at various distances below the nozzle exit.

Results

Shell formation.

Both the gas and the liquid issued from the nozzle in steady motion, but, because of instability, the flow became strongly periodic within a short distance from the nozzle exit. Fig. 3 shows four phases of the cyclic motion through which shells were formed. There, the velocity of the gas was three times that of the liquid. It is important to recognize that the volume flow rate of the gas therefore exceeded, by the same factor, the rate at which new volume was generated within the hollow core by the downward flow of liquid. The first frame depicts the free-surface configuration at the instant at which the liquid had sealed the core. On account of the larger volume rate of the gas, the gas of necessity produced a radial displacement of the cylindrical surface of the liquid, as in the second frame. The bulbous feature became progressively larger and more spherical, and was at the same time convected downward on a neck of liquid emerging from the nozzle, as in the third and fourth frames. The neck then collapsed under action of surface tension, completing the formation of a gas-filled nodule. Successive nodules of encapsulated gas produced in this manner were temporarily interconnected by a filament of liquid which broke subsequently, setting free the individual shells. None of the fill gas escaped.

A notable feature of this action is that the frequency stability of the process, estimated by stroboscopic observation, appeared to exceed one part in 10^3 . The motion was sufficiently definite that an attempt to alter the frequency by sinusoidal perturbation of the fill gas was unsuccessful. Moreover, even the details of the breakage of the filament were stationary; instantaneous oscillation waveforms induced upon the shells by the energy release, evident in figures described below, remained constant in appearance when viewed in stroboscopic light, and the ejection of satellite droplets, whenever present, was similarly constant. The motion was highly deterministic.

Analysis.

No analysis adequate to explain the shell formation process is known to be available at present. D. Weihs of Technion, Haifa, Israel (private communication) has performed a linearized, parallel-flow, analysis of a hollow jet and shown that, as in Rayleigh instability, a range of wave lengths is unstable. This result is in contrast with the present observation that a single frequency of oscillation is dominant. Evidently, a numerical analysis such as that described by Fromm³ will be required.

It may be appropriate here to consider the relative importance of various forces, and to present an analysis of a limiting case. The forces and stresses to be considered include the following:

Dynamic pressure of the gas,	$\rho_g v_g^2/2$
Dynamic pressure of the liquid,	$\rho_l v_l^2/2$
Viscous stress of the liquid,	$\mu_l v_l/r$
Capillary pressure,	$\sigma/r,$
Hydrostatic pressure,	$\rho_l g/r$

Here, ρ denotes density, V denotes velocity, μ denotes viscosity, σ denotes interfacial tension, G is gravity, and r is the jet radius. Subscripts g and l denote gas and liquid. A number of these stresses are generally or conditionally unimportant, as will be shown. On the basis of the formation cycle of Fig. 3, the forces which seem to be predominant are those of capillary pressure and of liquid dynamic pressure, and even the latter may be regarded as of secondary magnitude because the principal component of motion amounts to a uniform translation of the liquid. The motions with respect to this average one give form to the cycle, but do not induce substantial pressures.

The most important forces are evidently those due to capillary pressure. Accordingly, a static analysis has been made and found to provide a useful prediction of the shell diameter and of the formation frequency. Fig. 4 shows an idealization of the configuration present in the third frame of Fig. 3, consisting of a cylindrical neck joined to a spherical bulb. The reason that the spherical and cylindrical regions remain distinct is described below. The pressure required to support the cylinder against collapse is given by

$$p_c = \frac{2\sigma}{r_c},$$

where p_c and r_c are the pressure within, and the average radius of the cylinder. The factor, 2, accounts for the presence of the interior and exterior surfaces. The corresponding pressure for the sphere is

$$p_s = \frac{4\sigma}{r_s}.$$

The higher factor here results from the compound curvature of the spherical surface. It is to be noted that r_c is independent of time, whereas r_s is an increasing function of time. As the sphere fills, the pressure therein falls, and when the radius attains a value twice that of the cylinder the pressure becomes less than that required to prevent collapse of the cylinder. Therefore, according to this analysis, when the sphere attains a diameter twice that of the jet, its growth will be terminated by a sealing-off of the core. The frequency of formation may then be estimated in terms of the prevailing gas flow rate and the volume of each shell. It is to be noted that although the instability and shell formation process are surface-tension-driven, this parameter does not appear in the expression for the expected diameter.

This prediction of diameter was tested through measurement of the shell diameter and formation frequency as a function of flow rate. Fig. 5 presents this result in dimensional units. There, the measured diameter may be compared with the value expected from static analysis, shown as a horizontal line. Estimates of the interior and exterior radii of the surfaces were incorporated in forming the latter value, rather than the average. The measured shell diameters exceed the predicted value by approximately 10 percent, and do not fully verify the expected constancy in diameter. Nevertheless, the static analysis appears to have some merit. Also shown is the formation frequency, which possesses a one-third power dependence upon the flow rate. One important consequence of the frequency variation is that a measure of control may be gained over the wall thickness of the shells on account of the constancy of the liquid flow rate. Further control is to be had through adjustment of the dimension of the annular passageway of liquid flow.

Dynamic forces were responsible for preserving the demarkation between the spherical and cylindrication regions of the flow, since this could not have been maintained statically. It is believed that the abrupt change in surface curvature propagated in wave-like manner upward against the downflow of the jet, but with a velocity less than that of the liquid. An estimate of the wave speed has been made by considering the liquid to constitute a membrane, with transverse curvature being neglected. The wave speed, V_w , would be given by $(2\sigma/\rho_1\delta)^{1/2}$, where δ is the thickness of the layer, as in Fig. 4. The ratio of liquid velocity, V_l , to this velocity is then

$$\frac{V_l}{V_w} = \left[\frac{\rho_1 V_l^2 \delta}{2\sigma} \right]^{1/2},$$

a number found to exceed unity substantially in all successful tests, thereby indicating that a "supersonic" jet velocity is required for maintaining the spherical and cylindrical regions as distinct. For the case of small liquid velocities the bubble remained attached to the nozzle and grew to a diameter several times that of the orifice before bursting.

ORIGINAL PAGE IS OF POOR QUALITY

Further Experiments.

A number of experiments were carried out with the intention of exploring the regimes of operation and of assessing the relative importance of various forces and stresses. One such stress was the dynamic pressure of the gas. The expected unimportance of this quantity was verified by the finding that the bubble formation frequency and geometry were independent of gas composition for equal rates of flow of the gases, Freon 12, nitrogen, and helium, which span a density range 30:1. Also, the effect of the viscosity of the liquid, which may be characterized in terms of the Reynolds number, $\rho_1 v_{1r} / \mu_1$, was examined. It was found for the case of glycerin as the test liquid within the 4.0-mm nozzle that the formation process was changed little from that for water, which possesses 500-fold less viscosity. It is believed that Reynolds numbers in excess of 10^4 are adequate to ensure operation similar to that described.

It was pointed out that surface tension did not appear in the expression for shell diameter. This was tested by operating the 4.0-mm nozzle at constant flow of distilled water, to which was added in transient manner a surfactant (Kodak Photo-Flo). Fig. 6 compares the formation process before and after the addition of surfactant. Stroboscopy indicated that the frequency of formation diminished in consequence by approximately one percent, and an increase in diameter of one-third that amount must have occurred, but was not easily detectable. The most apparent difference in the two streams of the figure is a lesser degree of surface-wave activity upon the shells in the presence of surfactant. The waves were induced by the breakage of the interconnecting filament, and the energy released thereby must have been reduced by the lowering of the surface tension. The surfactant may have contributed to a damping of the motion as well as to the reduction in initial wave amplitude. As a general observation, the addition of surfactant improved the apparent quality of shells observed at a station one or two meters below the nozzle exit.

The effect of gas flow rate upon shell diameter and formation frequency was described above, and it was indicated that the gas volumetric flow rate must exceed that at which the liquid flow generates new volume within the core for successful operation. Fig. 6 shows the progression in flow geometry as the gas flow rate was increased for a constant liquid velocity. The three settings are characterized there in terms of the ratio of the gas-to-liquid velocities. For a ratio slightly above unity, shown in the first frame, a relatively long time interval was required to accumulate sufficient gas to form a shell, and the axial spacing between shells was large. It was found in this case that the configuration of the cylindrical neck was steady in time, that the motion of seal-off was confined to a region several diameters below the nozzle, and that the diameter of the shells was somewhat less than twice that of the nozzle. For a ratio of velocities near optimal, as in the center frame, the motion was as described previously, with the diameter being twice that of the nozzle. The third frame shows that for a high flow rate the shells exhibited the same 2:1 diameter ratio, but were produced at sufficiently short intervals as to remain interconnected for considerable distance, whereupon erratic coalescence was observed. The thinness of the shell wall may be seen.

As a further test of the range of operation, the liquid rate was increased four-fold with respect to that of the former figure, and the gas rate was advanced to approximately three times that of the liquid, or near optimal. The result is shown in Fig. 8, wherein the two frames at the right were obtained at higher magnification than that on the left, and differ only with regard to the phase of the cyclic motion. As seen, the water surface had assumed a very irregular form, and this is believed to have been due to an onset of fluid turbulence within the gas flow. The Reynolds number of the flow within the supply tube amounted to 5000, approximately, a value for which a turbulent condition is to be expected. Apparently, the unsteadiness of the turbulence induced capillary waves upon the free surface of the liquid. Even though this additional complexity was present, the shell-formation cycle remained similar to that shown before, with the shell diameter having been twice that of the nozzle.

As a test of nozzle geometry, the 4.0-mm nozzle was operated with air tubes whose diameters were as small as 1.2 mm. The spacing interval between nodules was large, as in the first frame of Fig. 7, because the gas flow was restricted. The interconnecting filament contained much of the liquid, and this was transferred to the shells upon breakage, rendering the walls thick.

Shell Symmetrization.

An important goal of the work was to produce rigid shells possessing a high degree of symmetry. Two aspects of this matter were considered. First, it was necessary to prevent the specimens from becoming distorted during the time interval following formation and preceding solidification. In particular, the shells were launched by the jet with a certain velocity, and tended to gain additional velocity by gravitational acceleration. The air resistance was found to produce a strong decentering force upon the captured gas, resulting in a localized

ORIGINAL FORM OF OF POOR QUALITY

thinning of the wall, and terminating in rupture. This type of distortion and failure were particularly severe for large shells, for which the dimensionless parameter characterizing gravitational effects, $\rho_1 Gr^2/\sigma$, was also large.

Control over this problem was gained by constructing a drop tower in the form of a vertical wind tunnel configured such that the airflow within it accelerated downward with a 1.0-G value. With proper placement of a shell generator therein, the specimens experienced no relative air velocity, and no decentering force. Fig. 9 shows a 7.0-mm H_2O shell photographed in free-fall in this tunnel at a location 2.0 m below the nozzle. The exterior surfaces of the shells were found to be spherical to within one percent. The white line appearing within the image circumference in Fig. 9 was determined through use of a ray-tracing program to represent the location of the interior surface of the shell. The wall thickness was thereby indicated to amount to ten percent of the radius and to be uniform to within ten percent. In the absence of the downflow, the shells ruptured before reaching this station of observation. As a means for determining whether the reduction in relative airflow would prevent the freezing of molten metal specimens, measurements were made of the temperature-loss of hot water shells. The heat transfer rate was found to exhibit a fairly sharp minimum when the airflow acceleration was adjusted to a 1.0-G value, but to retain more than half the rate prevailing when the mismatch was substantial. Although solidification of metal specimens has not been attempted here, difficulty on account of the magnitude of the heat transfer is not expected for the case of moderate shell sizes.

A second aspect of shell symmetrization concerned the promotion of centering by means of shell vibration. Theoretical and experimental studies on shell dynamics are given by Saffren, Elleman, and Rhim⁴. Included there are numerical results for shell vibration frequencies for the case of inviscid liquids, together with experimental results showing that such vibration has the beneficial effect of inducing a centering of the interior surface with respect to the exterior one. Also, Lee, Feng, Elleman, and Wang and Young⁵ show that the centering force attainable by means of forced oscillation is very strong. The present studies do not yet include results on centering by stimulated oscillation, but an observation of possible interest was made for the case in which surfactant was added to water. As mentioned, the initial level of shell oscillation induced by breakage of the liquid filament was greatly diminished then, and vibration was not detectable by eye at stations a few centimeters below the nozzle. Nevertheless, the centering of the surfaces was judged to equal that of the distilled water case.

Production of metal shells.

As indicated, metal shells may find application in inertial-confinement fusion technology. Such shells must be dimensionally precise, smooth, and strong. It has been shown here that the hollow-jet instability produces shells of great dimensional uniformity, that surface tension produced sphericity, and that forces not directly identified resulted in a concentricity of the surface. Work has been initiated on the use of liquid metals to form shells, and various aspects of this have been described by Kendall, Lee, and Wang⁶. The most successful results to date were obtained by Lee, who used a nozzle similar to that shown in Fig. 2. The metal employed was an alloy of gold, lead, and antimony which may, with adequate cooling rate, be solidified in the amorphous state. Certain properties of this metal, including that of surface smoothness, have been described by Lee, Kendall, and Johnson⁷.

Fig. 10 shows two shell specimens formed of this metal. The radiograph indicates that the wall thickness uniformity was good. The wall was sufficiently thin that the average density of this specimen was less than that of water. The SEM photograph on the right shows a shell which was broken at the time of recovery, thereby making visible the wall thickness and a portion of the interior surface. The cooling rate in this experiment was insufficient to attain the amorphous state, and surface imperfections are clearly evident on that account. Most liquid metal tests have involved tin or lead, rather than the alloy, and these have been found to model the flow of the alloy fairly well. Tin shells with diameters between 0.75 and 2.0 mm have been produced. A problem yet to be circumvented concerns the formation during solidification of an exterior surface protrusion at each of the locations from which a filament of liquid had been attached. This defect is apparently due to material properties or to heat transfer, and is not of fluid-dynamic origin.

Acknowledgements

This work represents one phase of research carried out at the Jet Propulsion Laboratory, California Institute of Technology, under Contract NAS 7-100 of the National Aeronautics and Space Administration. E. W. Miles and M. E. Lucero performed many of the observations reported here. G. E. Tennant fabricated the nozzle components. J. R. Gatewood provided extremely valuable advice on materials and techniques for the metal shell experiments.

ORIGINAL PAGE
BLACK AND WHITE PHOTOGRAPH

References

1. Lamb, H. "Hydrodynamics," 6th ed., Dover Publ. Co.
2. Hendricks, C. D., "Inertial Confinement Fusion Targets," Second International Colloquium on Drops and Bubbles, Monterey, CA, November 1981.
3. Fromm, J., "A Numerical Study of Drop-On-Demand Ink Jets," Second International Colloquium on Drops and Bubbles, Monterey, CA, November 1981.
4. Saffren, M., Elleman, D., and Rhim, W.-K., "Dynamics of Compound Drop Systems," Second International Colloquium on Drops and Bubbles, Monterey, CA, November 1981.
5. Lee, M. C., Fang, I-An, Elleman, D. D., Wang, T. G., and Young, A. T., "Generation of a Strong Core Centering Force in a Submillimeter Compound Droplet System," Second International Colloquium on Drops and Bubbles, Monterey, CA, November 1981.
6. Kendall, J. M., Lee, M. C., and Wang, T. G., "Metal Shell Technology Based upon Hollow Jet Instability," J. Vacuum Sci. and Tech., Mar. 1982 (to be published).
7. Lee, M. C., Kendall, J. M., and Johnson, W. L., "Spheres of the Metallic Glass $\text{Au}_{55}\text{Pb}_{22.5}\text{Sb}_{22.5}$ and their Surface Characteristics," Applied Phys. Letters, Mar. 1982 (to be published).

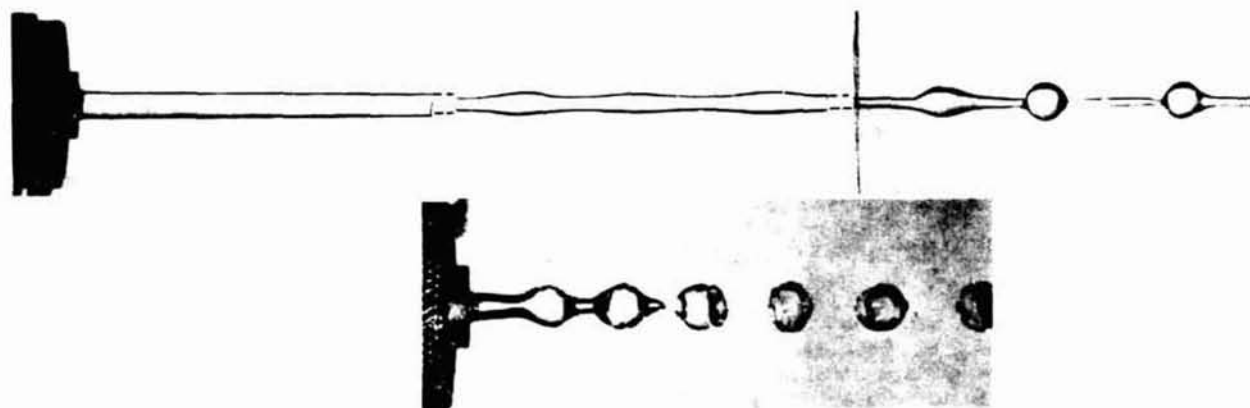


Fig. 1. Flow of water from a 4.0-mm nozzle; drops are produced by Rayleigh instability. Photographs obtained with 1.0-m axial spacing (upper). Same condition except for gas flow at core; shells are produced (lower).

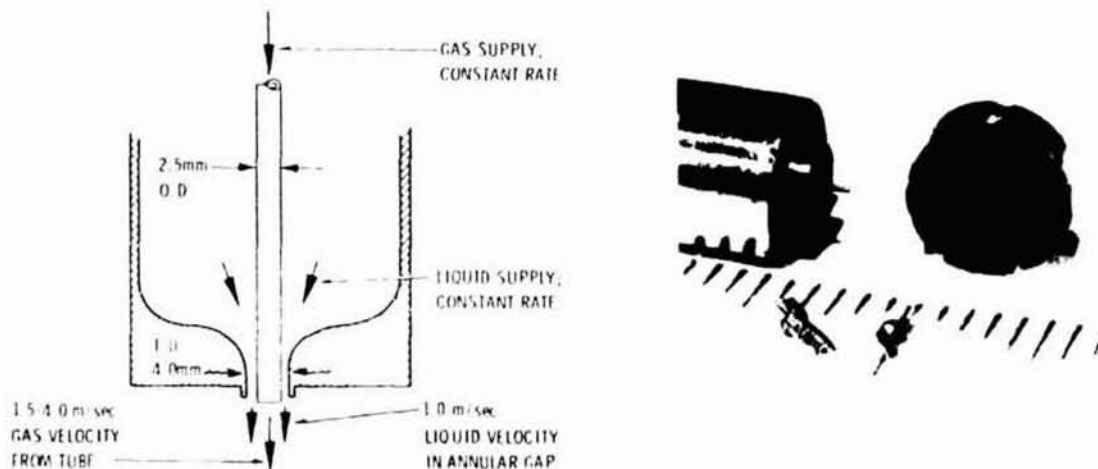


Fig. 2. Nozzle schematic, with typical flow conditions indicated (left). Photograph of a small nozzle, disassembled (right).

ORIGINAL PAGE
BLACK AND WHITE PHOTOGRAPH

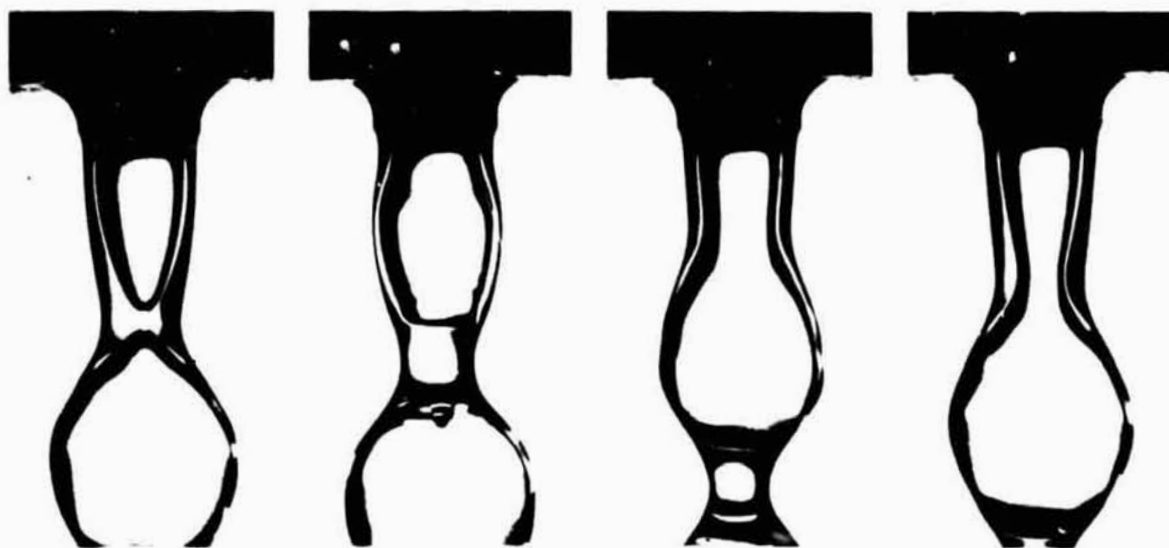


Fig. 3. Shell formation cycle.

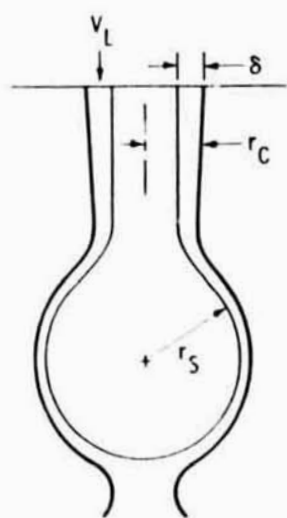


Fig. 4.

Idealization of liquid surface configuration.

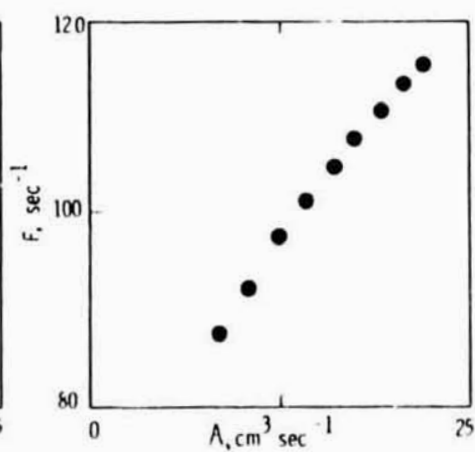
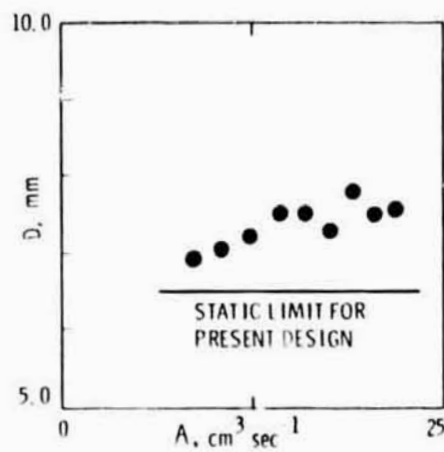


Fig. 5.

Shell diameter (left) and formation frequency (right) versus fill-gas flow rate for a 4.0-mm nozzle.

ORIGINAL PAGE
BLACK AND WHITE PHOTOGRAPH

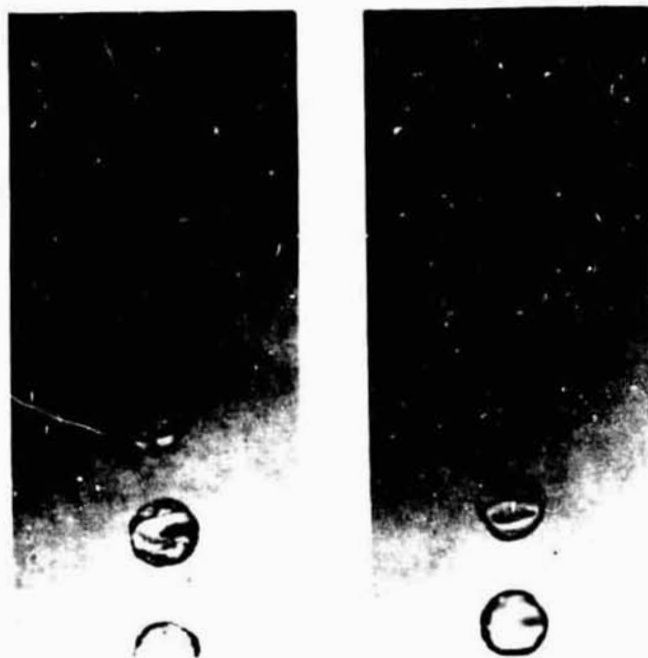


Fig. 6. Flow of distilled water from a 4.0-mm nozzle (left); same with surfactant (right).

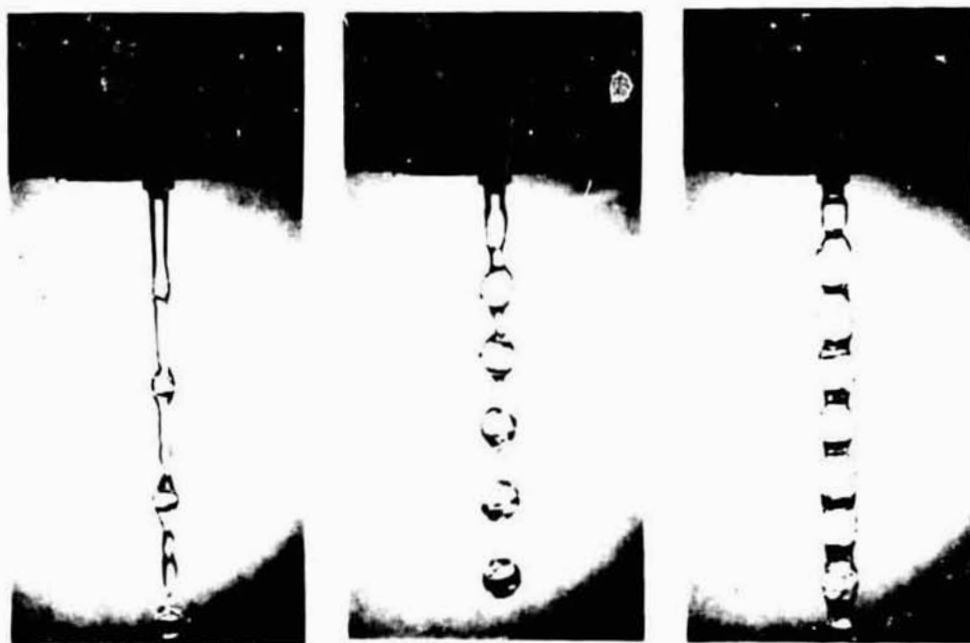


Fig. 7. Flow of water from a 4.0mm nozzle at $V_1 = 1.09$ m/sec. $V_g/V_1 = 1.4$ (left), 4.2 (center), and 12.6 (right).

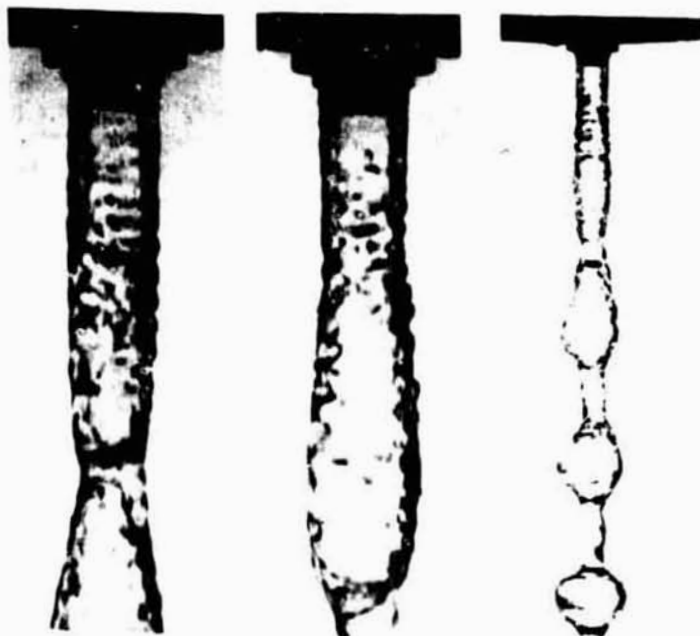


Fig. 8.

High velocity water flow from a 4.0-mm nozzle; $V_1 = 4.75$ m/sec;
 $V_2/V_1 = 3.0$; close-up view for two phases of motion (left,
(center); distant view (right).



Fig. 9.

7.0-mm diam. water shell with
surfactant; in free-fall.

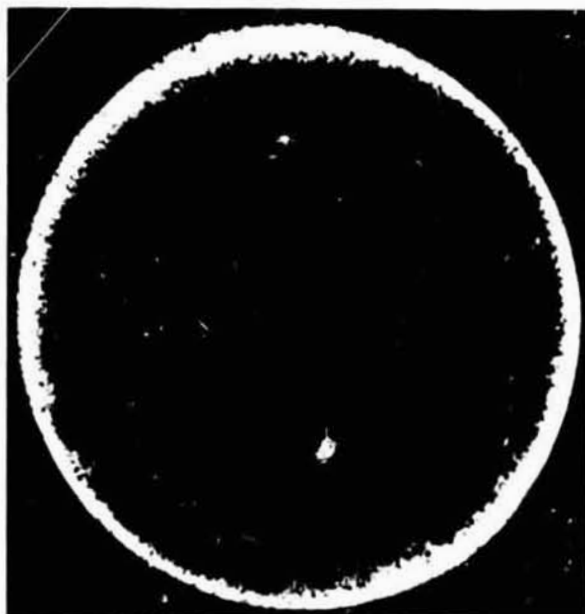


Fig. 10. Radiograph of an undamaged 1.5-mm gold alloy shell (left); SEM photo-
graph of similar shell except portion of surface is missing (right).